Title: Influence of repairable bolted dissipative beam splices (structural fuses) on reducing the seismic vulnerability of steel-concrete composite frames

Authors: Alper Kanyilmaz (Post-doc researcher, Politecnico di Milano), Milot Muhaxheri (Research fellow, University of Prishtina "Hasan Prishtina"), Carlo Andrea Castiglioni (Full professor, Politecnico di Milano)

ABSTRACT

After a strong earthquake, repair work of conventional steel-concrete composite buildings can be very expensive, and very often, impossible due to practical problems. Within the EU-funded research project FUSEIS, a new steel-concrete composite frame type has been developed, as a cost-effective and robust alternative to conventional earthquake resistant structures. In this new frame type, damage concentrates mainly in the bolted dissipative beam splices acting as "structural fuses", which can be easily and inexpensively replaced after strong seismic events. After the replacement, the building can be restored to its original form. This paper studies a benchmark building frame with and without bolted dissipative beam splices. The performance of both innovative and conventional structures has been quantified in terms of energy dissipation, floor displacements and inter-story drifts, as a result of nonlinear transient dynamic analysis. Different than similar studies in the literature, the numerical models explicitly consider the presence of reinforced concrete slab by means of fiber-based distributed plasticity approach. They have been calibrated according to the experiments, both provided in the literature and performed in the FUSEIS research project. The models allowed the quantification of the energy dissipated by each component of a steel-concrete composite frame (structural fuses, steel elements, concrete slab and steel reinforcement), which gave an insight on redistribution of dissipated energy in the case of adopting the structural fuses with respect to the traditional steel-concrete composite buildings. Based on the results of the numerical analysis, the reparability subject has been discussed.

Keywords: Composite steel-concrete frames, dissipative bolted beam splices, structural fuses, reparability, distributed plasticity

Acknowledgements

This article presents some of the outcomes obtained in the FUSEIS project, which was carried out with the financial grant of the Research Program of the Research Fund for Coal and Steel of the European Commission (Grant number RFSR-CT-2008-00032).

1 INTRODUCTION

Steel-concrete composite structural systems combine the two most common construction materials – steel and concrete – exploiting at best their mechanical properties. During the last decades, these structures have frequently been employed in the earthquake-prone regions. The earthquake events, such as US 1994 Northridge, 1995 Kobe, 2010 Chile and 2011 Christchurch gave important insights about their seismic behaviour. Even though not many global failures were apparent in case of steel-concrete composite buildings, the consequences were severe due to the widespread damage and local brittle failure of a large number of welded beam-to-column connections, and were associated with high repair costs (Engelhardt et al. 1997 [1]). An extensive number of laboratory investigation on connection and weldments (Engelhardt et al. 1995 [2]; Popov et al. 1996 [3]; Whittaker et al. 1996 [4]), and studies on fractured connections (Kaufman et al. 1995 [5]; Krawinkler, 1995 [6]) were conducted allowing to capture the leading causes of the connection damages related to both welding and design issues. These failures pushed the research community toward new design strategies to improve the seismic behavior of steel-concrete composite moment resisting frame connections. In the past, mainly two solutions were proposed to improve the seismic behaviour of steel-concrete composite frames: i) strengthening the joint (Krawinkler, 1995 [6]) ii) weakening the beam framing into the column, by reducing its section at a distance from the connections (Plumier A., 1990 [7], Yu et al. 2001 [8], Pachoumis et al, 2010 [9], Avgerinou [10]). Both solutions aim at “forcing” the formation of a plastic hinge in the beams away from the (welded) connection to achieve a better control of damages and to guarantee a ductile global behaviour, by also preventing a fragile collapse mechanism. This means that conventional systems, after a strong seismic event, are actually allowed to suffer significant inelastic deformations (permanent damages) in their main structural elements (steel beams and concrete slabs) and residual inter-storey drifts to a certain extent. Nevertheless, repair work in these cases causes a long interruption of functionality of the building, leading to extra costs and discomfort for building owners and occupants.

Several innovative dissipative technologies have been proposed for steel and composite steel-concrete structures (Engelhardt et al. 1995 [2]; Plumier A., 1997 [11]; Dubina et al. 2008 [12]; Chan et al. 2008 [13]; Gowda et al. 2013 [14]; Braconi et al. 2012 [15]; Piluso et. al 2014 [25]; Morelli et al. 2016 (a) [16]; Morelli et al. 2016 (b) [17]; Karavasilis T.L., 2016 [18]; Dall'Asta et al. 2017 [21]; Hwang et.al. 2017 [19]; Morelli et al. 2017 [22]; Vamvatsikos et al. 2017 [23], Latour et al. 2018 [24], Kamperidis et.al. 2018 [20]), which combine some of the most effective mechanisms for the dissipation of seismic energy input, obtained through the inelastic deformation of steel material. A comprehensive review of innovative dissipative systems and devices is presented by Vayas I. (2017 [26]), summarizing the results of a number of EU-RFCS projects carried out in the recent past, and rationalized within the EU-RFCS dissemination project INNOSEIS (http://innoseis.ntua.gr/ [27]). In the existing literature, mainly two aspects require further study regarding the structures with dissipative components. First, existing studies address most of the time the bare steel frame, ignoring the existence of the reinforced concrete slab. Therefore, experimental and numerical analysis to evaluate the performance of more realistic steel buildings with dissipative components are missing. Second, the researchers have so far mostly designed the dissipative systems to absorb as much energy as possible. However, although the damage reduction in the structural and non-structural elements after a disaster is a fundamental aspect for improving the long-term sustainability and resource conservation, the reparability aspect is generally ignored.

The need to restore damaged structural elements in post-seismic process has an increasing interest, as it concerns the reparability and the consequent costs that must be sustained for the repair works. Hence, while maintaining the benefits of high ductility necessary to perform the required deformations due to inelasticity, several studies have recently moved towards the research of new easily replaceable dissipative components.. In this perspective, the RFCS-funded project FUSEIS (Vayas et al. 2013 [28]; Calado et al. 2013 [29]; Castiglioni et al. 2012 [30]; Dimakoyianni et al. 2015 [31]; Dougka et al. 2014 [32]) introduced an innovative dissipative system for steel-concrete composite frames. This new connection type is achieved by introducing a discontinuity in the composite beams of a moment resisting frame and splicing the two parts of the beam through steel plates bolted to the web and flange of the beam. In what follows, the expression “structural fuse” will be often used as synonymous of “bolted dissipative beam splice”.

The configuration of the structural fuse inside a typical beam-to-column connection is shown in Figure 1. In this configuration, the plasticization is expected to take place only in the replaceable parts of the connection. The part of the column near to the connection is reinforced in order to obtain an adequate over-strength. With this connection configuration, the center of rotation of the fuse is placed between the two reinforcement layers, which promotes the buckling of the web and flange steel plates of the splice. This becomes the source of the energy dissipation of the replaceable beam splice without damaging the rest of the main steel elements of the structure.

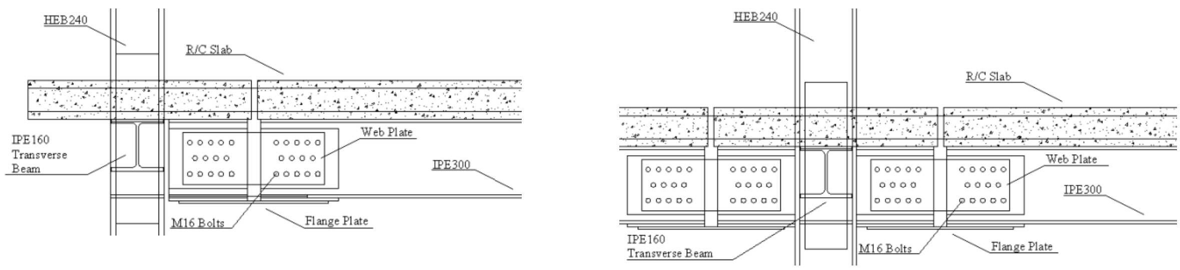

a. Exterior Beam-Column Joint Detail   b. Interior Beam-Column Joint Detail

Figure 1 Details of structural fuses (Castiglioni et al. 2012)

In the fuse section, a gap of 50 mm is left without interrupting the steel reinforcement bars, to avoid the damage to the concrete slab due to crushing under flexural deformation. This gap also aims to avoid damage to the floor finishes such as tiles, hydraulic piping or electric wiring. In everyday practice, the gap could be filled with low stiffness foams made of polymers which would not affect the structural performance, while in the other hand would guarantee covering/finishing continuity. These components in practice, may be designed referring to the existing EN1993-1-1 and EN1998-1-1, since all the elements included in the structure are made of classical steel construction components, unlike more technological devices (for example the seismic isolation devices) that need to be certified according to EN15129 to be used in practice (Vayas I., 2017 [26]).

In FUSEIS research project, beam-to-column joint components (Figure 2.a) and full scale specimens (Figure 2.b) have been tested respectively at Instituto Superior Tècnico of Lisbon and at Politecnico di Milano. The tested systems showed very good performance in terms of stiffness, ductility, energy dissipation and resistance, and the structural fuses proved to be very easily replaceable (Castiglioni et al. 2012 [30]). The main structural elements being the non-replaceable parts remained generally in the elastic range or with non-significant damages as intended. The inelastic deformation was mainly concentrated on the structural fuses that were the only component to be replaced after each test. The detailed findings obtained were presented in two articles (Castiglioni et al. 2012 [30]; Calado et al. 2013 [29]).

a. Component tests – IST b. Full scale tests - POLIMI

Figure 2 Experimental Set-up

This paper quantifies the performance of a benchmark multi-storey building with a steel-concrete composite frame designed by (Zona et al. 2008 [33]) with and without structural fuses by means of nonlinear transient dynamic analysis. Numerical models have been developed using distributed plasticity approach (Uriz et al. 2008 [34]; Sabelli R., 2001 [35]). The models have been calibrated with reference to the experimental results available in the literature (Nie et al. 2003 [36]; Bursi et al. 2000 [37]; Nie et al. 2011 [38]) and experimental investigations from the FUSEIS research project (Vayas et al. 2013 [28]). Global response parameters have been quantified such as energy dissipation, base shear and inter-storey drifts.

2 SIMPLIFIED STEEL-CONCRETE COMPOSITE FRAME MODEL

Parametric analysis of the structural fuses was performed with refined finite element numerical models in previous studies (Valente et al. 2016 [39]; Valente et al. 2017a [40]; Valente et al. 2017b [41]), which can be used for specific research applications. However, to study the performance of whole building structures, a simplified model has been proposed hereafter and validated against experimental results from previous studies. The finite element model has been developed using fiber-based beam elements with distributed plasticity implemented in Strand7 environment (Strand7 2004 [42]). This modelling approach distributes plasticity by numerical integrations using mainly the displacement-based finite elements: each element is divided into several cross sections along the member length, which are further subdivided into fibers with specific stress/strain relations (Nguyen et al. 2014 [43]). The fibers are considered as mono-dimensional elements with nonlinear elastic constitutive law. Assuming that plane sections remain plane, the strain in each fiber is calculated from centroidal section strain and curvature, then the stresses are calculated from the previous strain values. By integrating the response of the fibers, the constitutive relation of the cross section is obtained, which is then integrated along the member length and allow monitoring the axial force and moments, incremental moment-curvature and axial force-strain relations. Finally, nonlinear transient dynamic analysis has been performed, considering material and geometrical nonlinearities, for the beam and column elements, and plastic links for fuse elements.

The modelling of the concrete nonlinear behaviour is characterized by the complexity of the material features, such as mechanical parameters degradation, energy dissipation for hysteresis, progressive cracking caused by tensile stresses and strains. Moreover, the presence of reinforcement requires more complex modelling considerations such as: bond between concrete and steel, aggregation interlocks and dowel action. Since the aim of this study is the investigation of the global response of a building structure where the presence of concrete material is limited to the slab of the composite beam, and to achieve a high calculating efficiency, a simplified stress-strain relationship for plain concrete in the uncrushed and un-cracked condition has been considered. In this regard, a conservative set of rules are applied for the definition of stress-strain relationship on post-peak phase, by omitting the decreasing stress value for the definition of the softening branch. It is worth emphasizing that the softening and localisation problems, which could be regarded as material instabilities that are caused by micro-cracks, are considered not to affect the macrostructure behaviour at a significant level. Up to the peak, the parabolic curve equation from (UNI EN 1992 2004 [44]) Eqs. (1-4) has been used, and a constant branch has been considered after reaching the peak compressive strength (Figure 3.a).

$$\frac{\sigma_c}{f_{cm}} = \frac{k \cdot \eta - \eta^2}{1 + (k-2) \cdot \eta} \qquad \text{(eq.1)}$$

where:

$$- \ \eta = \frac{\varepsilon_c}{\varepsilon_{c1}} \qquad \text{(eq.2)}$$

$$- \ k = 1{,}05 \cdot \frac{E_{cm} \cdot |\varepsilon_{c1}|}{f_{cm}} \qquad \text{(eq.3)}$$

$$E_{cm} = \left(\frac{f_{cm}}{10}\right)^{0.3} \qquad \text{(eq.4)}$$

For concrete in tension, the adopted constitutive relation consists in two parts: the first one is linear elastic up to the tensile strength f_{ctm} Eq. (5) and a strain equal to 0.0015%; then a pure plastic behaviour with a constant branch has been considered.

$$f_{ctm} = 0.4 f_{ck}^{2/3} \qquad \text{(eq.5)}$$

The steel constitutive relationship is idealized as a bilinear curve, representing elastic-plastic behaviour with linear strain hardening (Figure 3.b), symmetric both in tension and compression. In order to verify the proposed numerical models and investigate the nonlinear behaviour of the composite frame structure, some examples from the literature, including simply supported beams and plane frames, were analysed and compared with the respective experimental results.

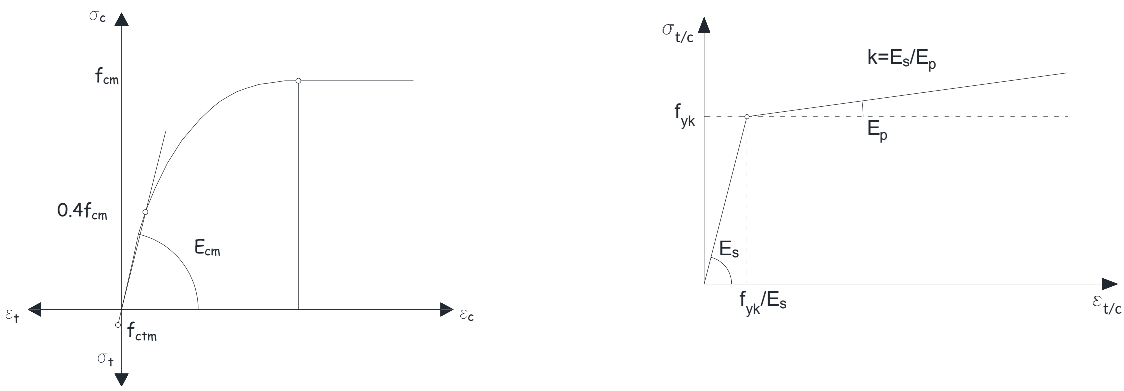

a. Concrete Stress-Strain relationship b. Reinforcing Steel Stress-Strain relationship

Figure 3 Steel constitutive relation

2.1 Steel-concrete composite slab

To achieve a good balance between the numerical accuracy and feasible computational time, a simplified model has been developed for the steel-concrete composite connections used in this study. The numerical model is schematically represented in Figure 4. Steel beams and columns reinforced concrete slab and structural fuse are modelled with two-node fiber beam elements. Slip effect between the steel beam and concrete slab is not considered since its influence on the global response of the building is assumed to be not significant in this case. Therefore, the overlaid beams sharing the same nodes have the same translation and rotation degree of freedoms. This full composite action has been represented by rigid link elements connecting the steel and concrete beam elements (simulating the shear connectors). An additional beam element has been used to simulate the two rows of steel reinforcement, placed at the centroid of the concrete slab. The distance between the centroids of the concrete and the steel beam is taken into account applying an offset to the concrete slab element.

In the performance of the buildings with steel-concrete composite frames and structural fuses, since most of the plasticity concentrates in the fuses. the impact of the phenomena such as strength deterioration of the concrete and the contact between concrete slab and steel column should be minimal. Therefore, during modelling, these two phenomena are not considered, resulting in a more robust steel-concrete composite connection with slightly underestimated energy dissipation capacity. For the comparison purposes of this paper (performance of the buildings with and without fuses), these simplifications can be acceptable since in both cases the same imperfections will be present. Finally, the accuracy of the models are rated using the experimental results of the tests in the literature, performed with simply supported beams (i) (Nie et al. 2003 [36]) continuous beams (ii) (Bursi et al. 2000 [37]), and plane frames (iii) (Nie et al. 2011 [38]).

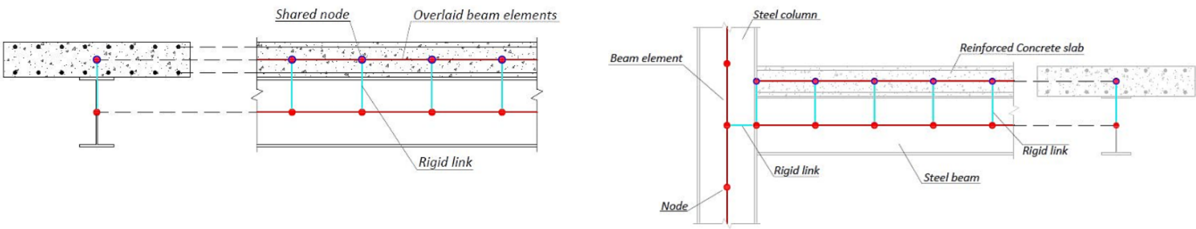

a. Section view   b. Front view

Figure 4: Numerical model scheme of composite steel-concrete beam.

2.1.1 Simply-supported composite beam tested by (Nie et al. 2003 [36])

In order to verify the rationality of the adopted numerical model, the nonlinear behaviour of a simply-supported composite beam has been simulated under monotonic loading. The specimen was subjected to hogging moment (Nie et al. 2003 [36]). Two models are developed, namely with and without slab reinforcement. The cubic compressive strength $f_{ck,cube}$, reinforcing steel yield strength f_{yr} and structural steel yield strength f_{ys} are adopted from experimental results reported as 27.7 N/mm^2, 290 N/mm^2 and 310 N/mm^2, respectively. The deformed shape under sagging visualized together with yield ratio shows that the concrete slab is mainly under compression; thus, the results are insensitive whether, in the model, the slab reinforcement is considered or not (Figure 5).

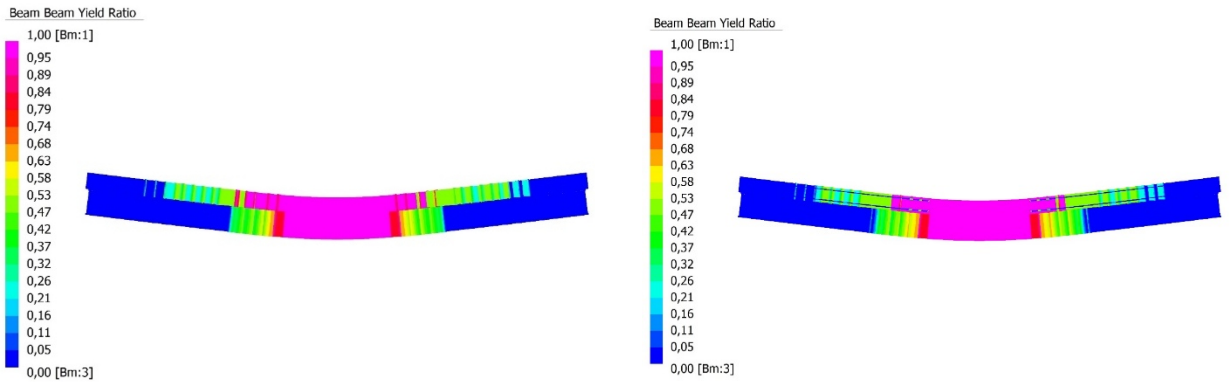

a. Without reinforcement. b. With reinforcement.

Figure 5 Deformed shape with yield ratio of simply-supported composite beam tested by (Nie et al. 2003 [36])

The results show that the simplified numerical model captures tolerably the test specimen behaviour as concerns the initial stiffness and moment capacity; the presence of slab reinforcement does not affect the result in terms of stiffness, but slightly influence the ultimate flexural capacity, as shown in Figure 5 and presented in Table 1.

	Numerical	**Experimental**	**Ratio Num/Exp**
Stiffness (kNm/m)	14433	12998	1,11
M_{yield} w/o reinforcement (kNm)	147	125	1,18
M_{yield} with reinforcement (kNm)	147	125	1,18
M_{max} w/o reinforcement (kNm)	202	199	1,02
M_{max} with reinforcement (kNm)	207	199	1,04

Table 1 Quantitative comparison with (Nie et al. 2003 [36])

2.1.2 Composite frame joint tested by (Bursi et al. 2000 [37])

The nonlinear behaviour of the composite frame tested by (Bursi et al. 2000 [37]) has been simulated under cyclic loading. The cylindrical compressive strength f_{ck}, reinforcing steel yield strength f_{yr} and structural steel yield strength f_{ys} are adopted from experimental results reported as 39 N/mm^2, 482 N/mm^2 and 291 N/mm^2, respectively. The deformed shape under monotonic loading together with yield ratio are shown in Figure 6.

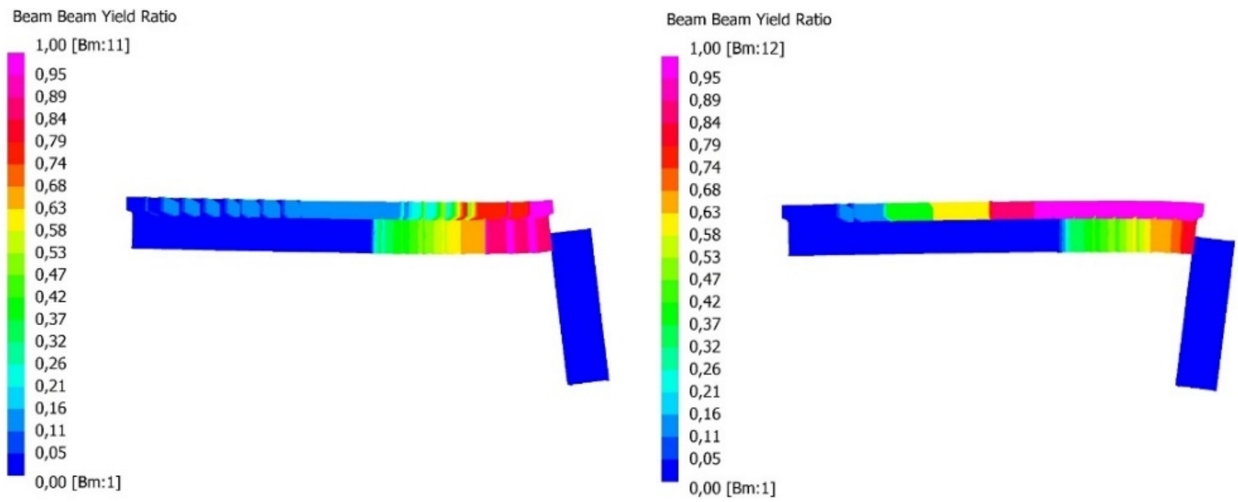

a. Pull b. Push

Figure 6 Yield ratios of the numerical model (Pull and Push)

The results of the cyclic loading show that the numerical model correlates adequately with the test specimen behaviour as concerns the initial stiffness (K_{push}, K_{pull}) and resistance ($F_{pull,max}$, $F_{push,max}$). The quantitative comparison is given in the following Table 2.

	Numerical	Experimental	Ratio (Num/Exp)
K_{push} (kN/m)	15849	15769	0.99
K_{pull} (kN/m)	17780	17004	1.05
$F_{pull,max}$ (kN)	355	359	0.98
$F_{push,max}$ (kN)	-236	-276	0.86

Table 2 Quantitative comparison (Bursi et al. 2000 [37])

2.1.3 Full scale composite frame tested by (Nie et al. 2011 [38])

The nonlinear behaviour of the composite frame tested by (Udagawa et al. 1991 [45]) has been simulated under cyclic loading. The cylindrical compressive strength f_{ck}, reinforcing steel yield strength f_{yr} and structural steel yield strength f_{ys} are adopted from experimental results reported as 22,6 N/mm², 300 N/mm² and 353.3 N/mm², respectively. The deformed shape under pull and push visualized together with yield ratio are shown in Figure 7.

	Numerical	Experimental	Ratio (Num/Exp)
Kpush (kN/m)	14010	13500	1.03
Kpull (kN/m)	14010	13500	1.03
$Fpull_{,max}$ (kN)	208	231	0.90
$Fpush_{,max}$ (kN)	-224	-236	0.95

Table 3 shows the comparison of results, which are in good agreement also in this case.

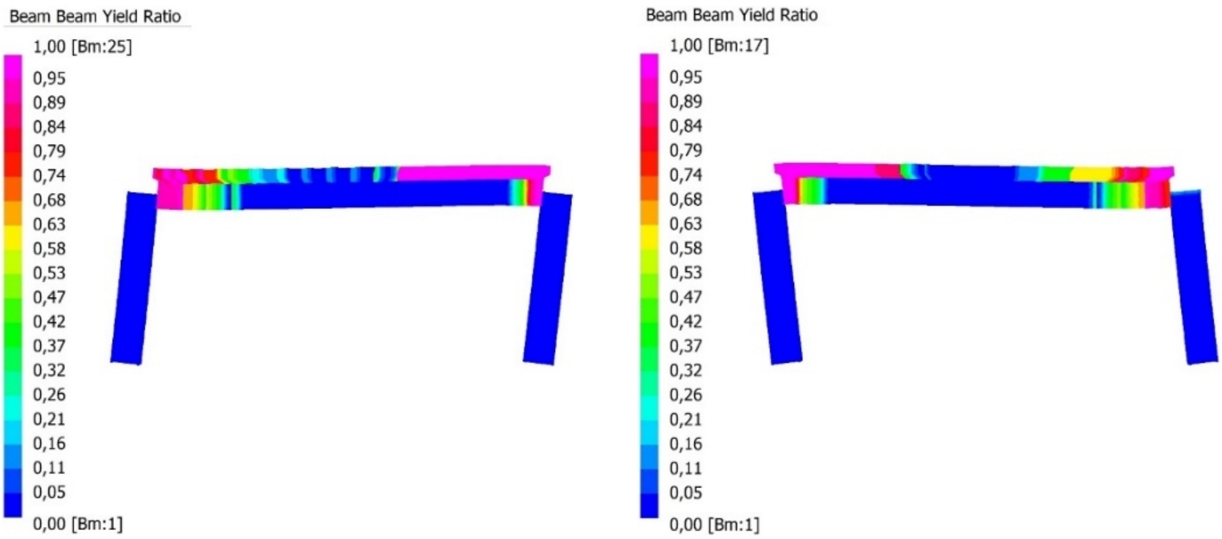

a. Pull b. Push

Figure 7 Yield ratio of numerical model (Push and Pull)

	Numerical	Experimental	Ratio (Num/Exp)
K_{push} (kN/m)	14010	13500	1.03
K_{pull} (kN/m)	14010	13500	1.03
$F_{pull,max}$ (kN)	208	231	0.90
$F_{push,max}$ (kN)	-224	-236	0.95

Table 3 Quantitative comparison (Udagawa et al. 1991 [45])

3 STEEL-CONCRETE COMPOSITE FRAMES WITH STRUCTURAL FUSES

Two numerical models have been developed to simulate the component and the full-scale cyclic tests implemented at Instituto Superior Tecnico (IST) in Lisbon (Calado et al. 2013 [29]) and at Politecnico di Milano (Castiglioni et al. 2012 [30]). The component test model aimed to characterize the fuses in terms of moment rotation curves, and the full-scale model intended to simulate a real scale case which was a portion of a storey of a composite steel frame with structural fuses. In the following, the details of these models are provided.

3.1 Numerical simulation of the component tests

The numerical model developed for the bolted structural fuse is shown in Figure 8.b. Steel columns and beams, concrete slab, and reinforcement steel are modelled with fiber-based inelastic beam elements. The structural fuse is modelled as a connection-beam element, positioned within the free length $L_0 = 170\ mm$, and connected to the adjacent beam elements with rigid links. The beam element representing the concrete slab has been introduced with an offset. The model has been developed based on the geometry used in the experimental set-up. To consider the reinforcing contribution of welded steel cover plates, the web dimension of the beam elements next to the connection have been increased by the thickness of the plates. Because of the presence of web stiffeners, the beam-to-column web panel area has been modelled with rigid links.

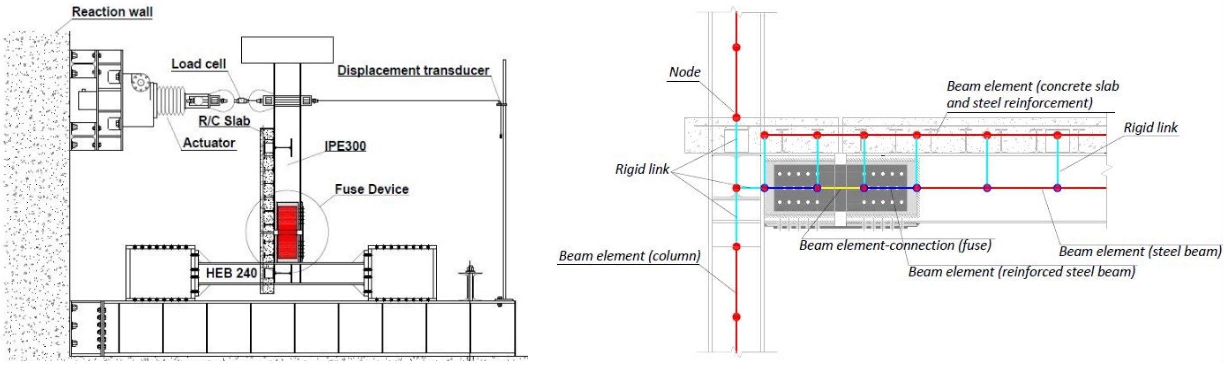

a. Component test set-up b. Numerical model of innovative joint

Figure 8 Experimental test set-up (Calado et al. 2013 [29])

As concerns the boundary conditions, the end nodes of the column are fully restrained while the top of the steel beam is free to move and subjected to an imposed displacement, in order to reproduce the cyclic loading history from the test. All the structural elements are modelled with elasto-plastic material. The uniaxial stress-strain relationship are based on the material properties reported in (Calado et al. 2013 [29]). Both structural and reinforcing steel are defined with a bilinear relation and kinematic hardening type, while the concrete is defined with a parabolic and linear branch in compression and with a linear and straight branch in tension, as described in section 2. The stress-strain curves are depicted in Figure 9.

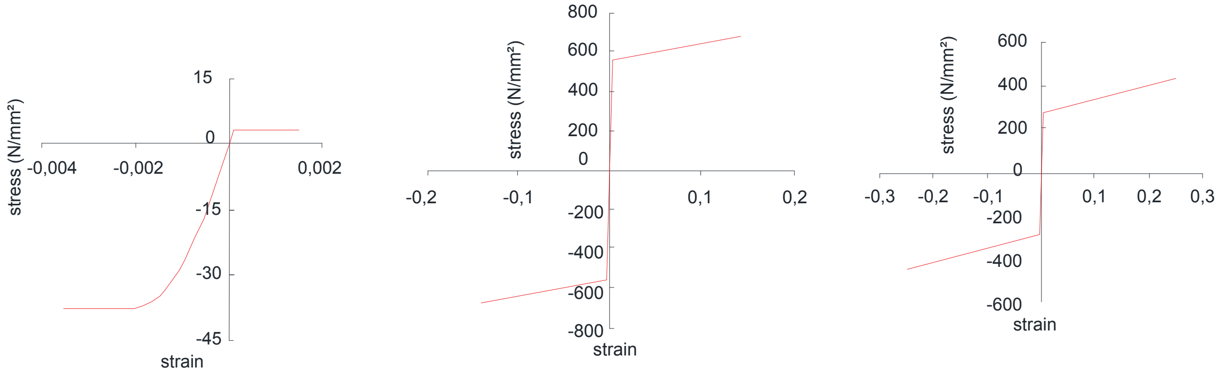

a. Concrete b. Steel reinforcement c. Structural steel

Figure 9 Material uniaxial stress-strain curve

The nonlinear behaviour of the connection element, representing the structural fuse, is defined by a moment-rotation diagram, which is calculated analytically, and calibrated according to the results of the component tests performed during FUSEIS research project (Vayas et al. 2012 [46]). In order to capture the nonlinear response, the hysteresis type is assumed to be the one described by the Takeda Model (Takeda T., 1970 [47]), which represent the most suitable hardening type among those provided by the numerical analysis software (Straus7 2004 [42]). Three models have been created, one per each fuse type considered (A, B and C in Table 4), which differ in terms of the flange height and thickness, while the web plate has the same dimension in all the tests. The moment-rotation input diagrams are reported in Figure 11.

Flange plate	A	B	C
t_f [mm]	10	10	12
b_f [mm]	120	170	150

Table 4 Dimensions of the flange plates

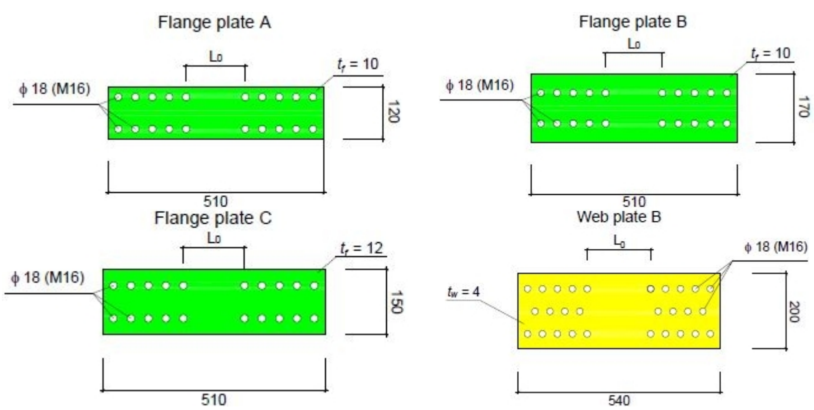

Figure 10 Dimensions of the fuse flange and web plates

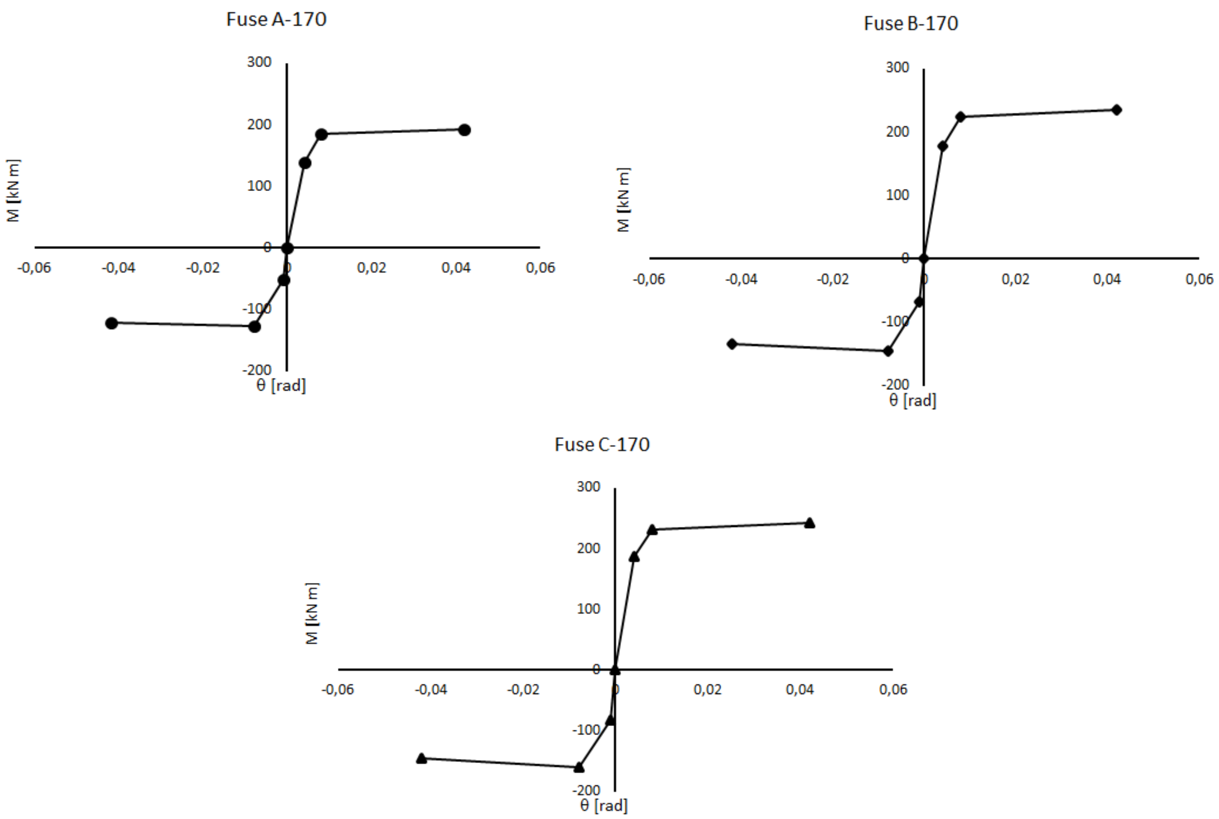

Figure 11 Moment-rotation input diagram for structural fuses

Figure 12 shows the comparison between the numerical and experimental results. While the steel beam and column remain within their elastic range, the overall joint behavior is characterized by the inelastic deformation taking place mainly in the structural fuses.. The asymmetry of the moment-rotation diaphragms is due to the configuration of the structural fuse composed of steel plates and composite steel-concrete slab. The maximum rotation observed in the structural fuse was 40 mrad. It can be observed that the amplitude of the hysteresis cycles obtained numerically are smaller, and this can be associated to the simplifications introduced in the definition of stress-strain tables and modelling assumptions. In all the cases, numerical results remain on the conservative side showing less energy dissipation with respect to the experiments Table 5. The best fit is achieved in the case of Fuse B.

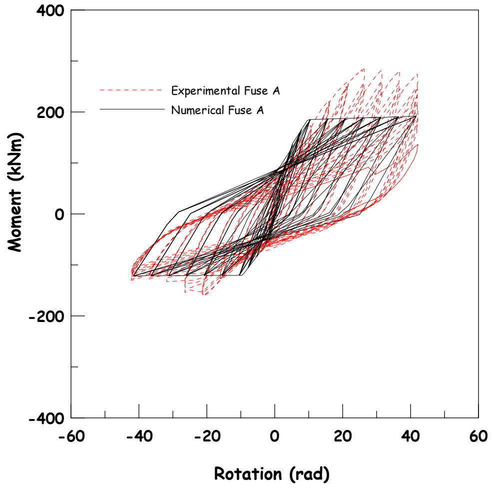

a) Fuse A

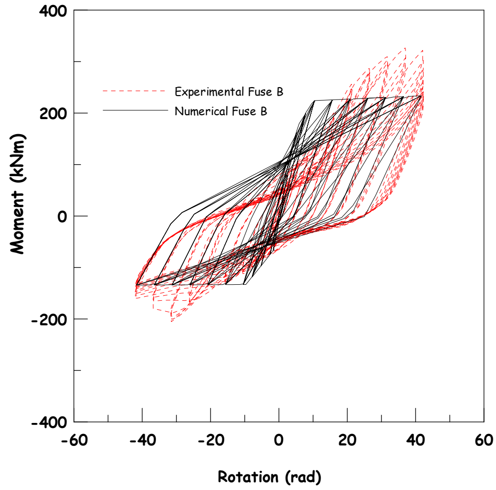

b) Fuse B

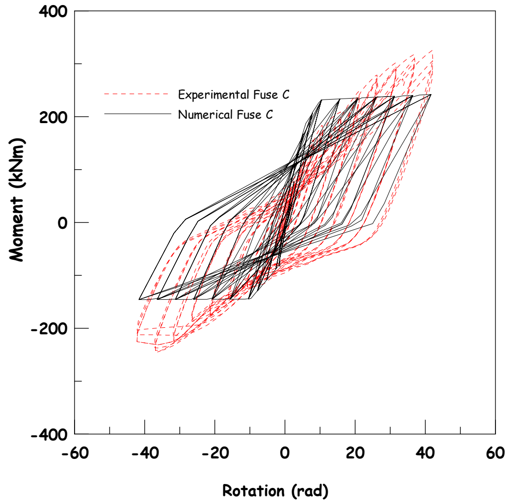

c. Fuse C

Figure 12 Experimental vs. numerical result of test specimen (Calado et al. 2013 [29])

Fuse	Experiments (kNmrad)	Numerical (kNmrad)	Ratio num/exp
A	13852	11525	0.83
B	14506	13700	0.94
C	15908	14456	0.91

Table 5 Total Energy Dissipation (Calado et al. 2013 [29])

The specimen after testing is shown in Figure 13. During sagging, flange and web plates were under tension, while under hogging, both plates buckled under compression. The composite beam and the column remained almost elastic with no evidence of plastic deformations in steel elements, and almost no tensile cracks in the concrete slab.

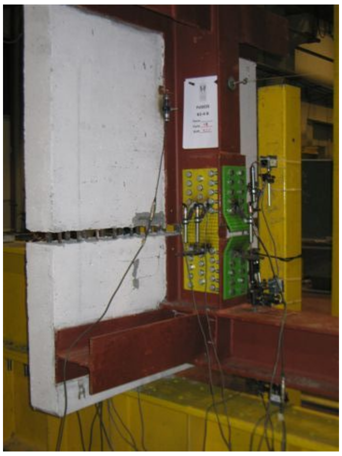

Figure 13 Inelastic deformation obtained during tests

3.2 Numerical modelling of the full-scale test specimens

The experimental set up (Figure 14) for the full scale test performed at Politecnico di Milano represents a portion of a multi-story frame, with three structural fuses namely Fuse 1, Fuse 2 and Fuse 3. The structure is composed of four HEB240 steel columns, two IPE300 steel beams and a 150-mm thick reinforced concrete slab supported by IPE160 transverse beam placed every 1.4 m, in addition to a pair of transverse beams, placed at each beam-to-column connection. Full shear connection is provided between the slab and the steel beam by means of IPE100 sections welded on top of the beam flange, acting as shear studs. The numerical model of the full-scale test specimens is developed assuming the same choices done for the component test specimen (Figure 8.b) as concerns the materials and geometry of the members and the moment-rotation input diagram of the fuses devices. The boundary conditions reproduce the experimental configuration: at the bottom, the columns are pinned while at the top, the rigid beam is modelled by enforcing the same displacement at both columns. The end node of the steel beam connected to the Fuse 3 is restrained only against vertical displacement with a roller. Three models have been created, one per each fuse type considered (A, B and C, see Table 4).

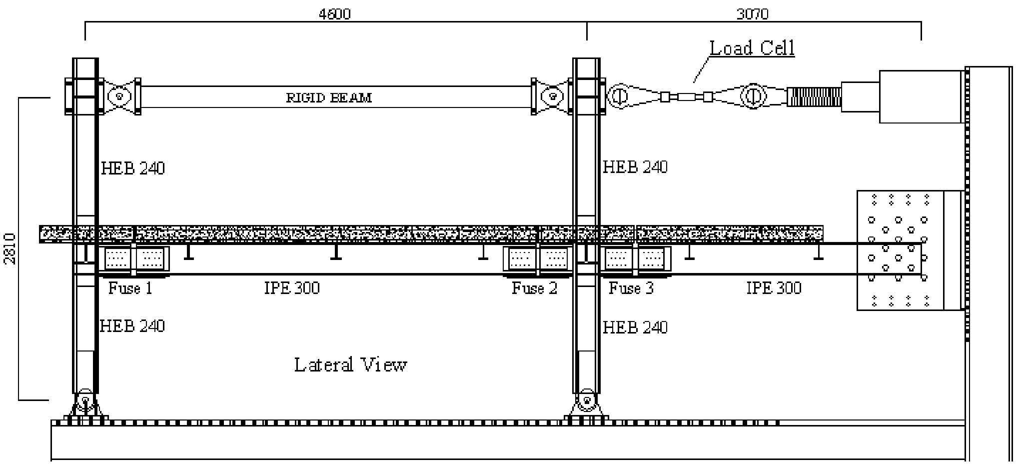

Figure 14 Experimental set-up (Castiglioni et al. 2012 [30])

Also, in this case, the inelastic deformation took place mainly in the structural fuses, the steel beams and columns remaining elastic. The maximum rotation observed in the structural fuse was 42 mrad. The comparisons between numerical and experimental results in terms of global force-displacement behaviour are shown in Figure 15. As in the case of component models, the amplitude of hysteresis cycles of the numerical models is smaller because of the simplifications introduced in the modelling. Numerical results remain on the safe side showing less energy dissipation with respect to the experiments Table 6.

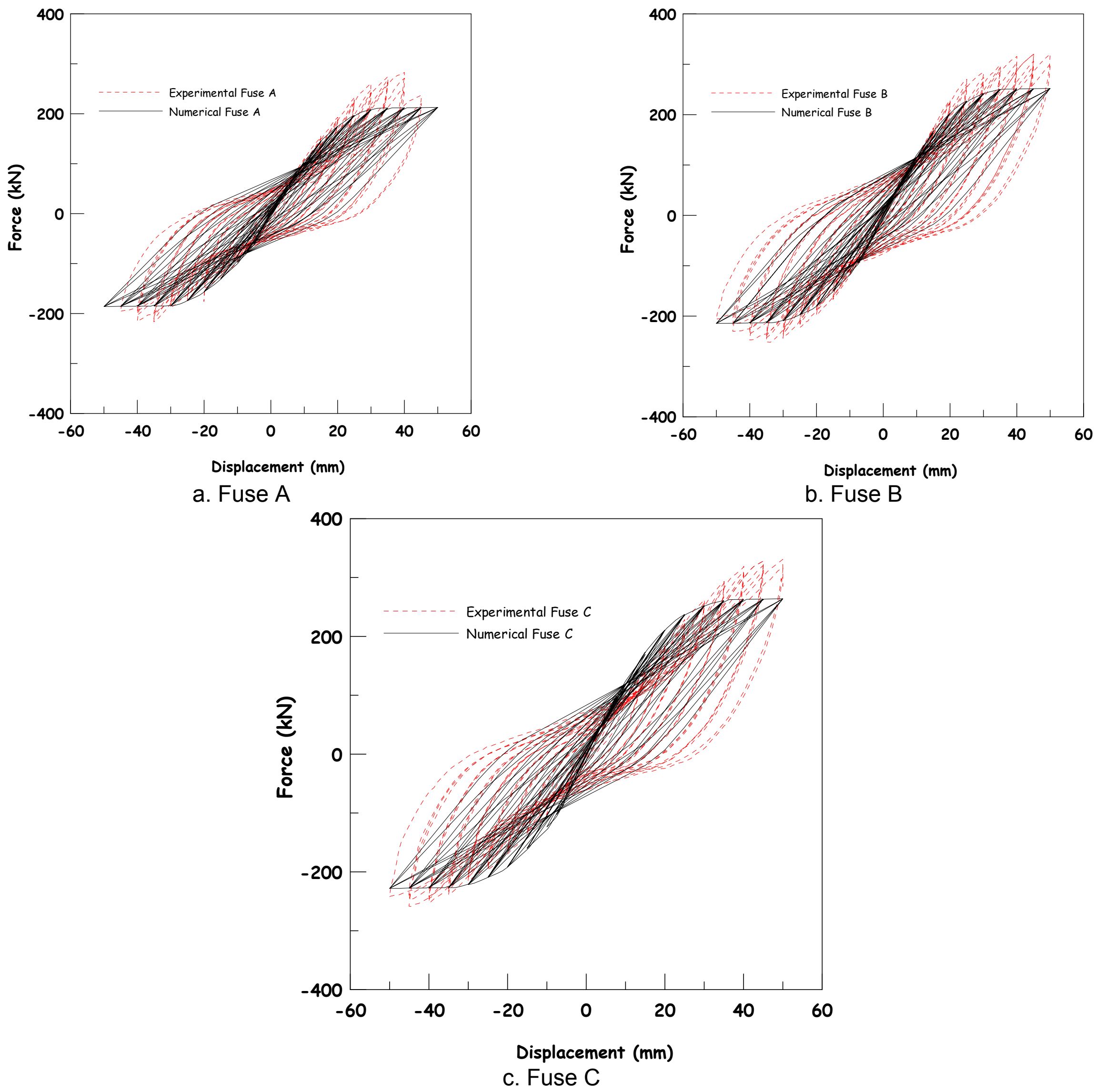

Figure 15 Experimental vs. numerical result for the test specimen (Castiglioni et al. 2012 [30])

Fuse	Experiments (kNmm)	Numerical (kNmm)	Ratio num/exp
A	13742	11523	0.84
B	19376	13238	0.68
C	17601	13973	0.79

Table 6 Total Energy Dissipation (Castiglioni et al. 2013 [30])

The inelastic deformation that provided the hysteresis behaviour can be seen in Figure 16 in case of an exterior (a) and an interior joint (b).

a. Exterior connection b. Interior connection

Figure 16 Inelastic deformation of the structural fuses

In general, the numerical models provide reasonable results. However, in some cases they result in lower energy dissipation with respect to the experimental ones. This is because of the simplifications introduced in the models to be able to achieve a feasible computational time for the nonlinear transient analysis of the multi-storey building example that is presented in the next chapter. Indeed, the objective of this study is not to simulate perfectly the steel-concrete composite structures which was already done in the previous studies (Nie et al. 2003 [36]; Bursi et al. 2000 [37], Valente et al. 2016 [39]), but to quantify the improvements obtained thanks to the structural fuses in the performance of the whole buildings with steel-concrete composite frames under acceleration-time history input.

4 STRUCTURAL FUSES IN A BENCHMARK BUILDING EXAMPLE

To quantify the performance of the structural fuses, two models have been analysed:

i) A conventional moment resisting steel-concrete composite frame (benchmark);
ii) A model with the structural fuses, placed close to the ends of composite beams of the benchmark model

Nonlinear time-history analyses have been performed. The results have been interpreted in terms of floor displacements, inter-story drifts, base shear and energy dissipated by each component of the steel-concrete composite frame (structural fuses, steel elements, concrete slab and steel reinforcement).

The benchmark model ("Model-B") is a five-storey two-bays moment resisting frame made of steel columns and composite beams, which was designed by (Zona et al. 2008 [33]) in a previous study (Figure 17). Each bay and storey has a span of 5 m and a height of 3 m. The steel columns are made of European HEB 300 wide flange S275 steel beams, while the composite beams are made of European IPE 270 S275 steel I-beams connected by means of stud connectors to a 100-mm-thick C25/30 concrete slab with an effective width estimated as 800 mm. The reinforcement of the concrete slabs consists of top and bottom layers of 400 mm^2 of B450C re-bars with a concrete cover of 30 mm. The frame was designed according to (UNI EN 1994-1-1 2004 [48]) to resist the static loads (composite cross section self-weight= 2.36 kN/m, permanent load G= 16 kN/m, and live load Q= 8 kN/m, uniformly distributed along the composite beams), and seismic forces were evaluated using response spectrum analysis with peak ground acceleration=0.35 g, Type 1 spectrum of (UNI EN 1998-1-1 2005 [49]), modal damping ratio=5%, and soil class B.

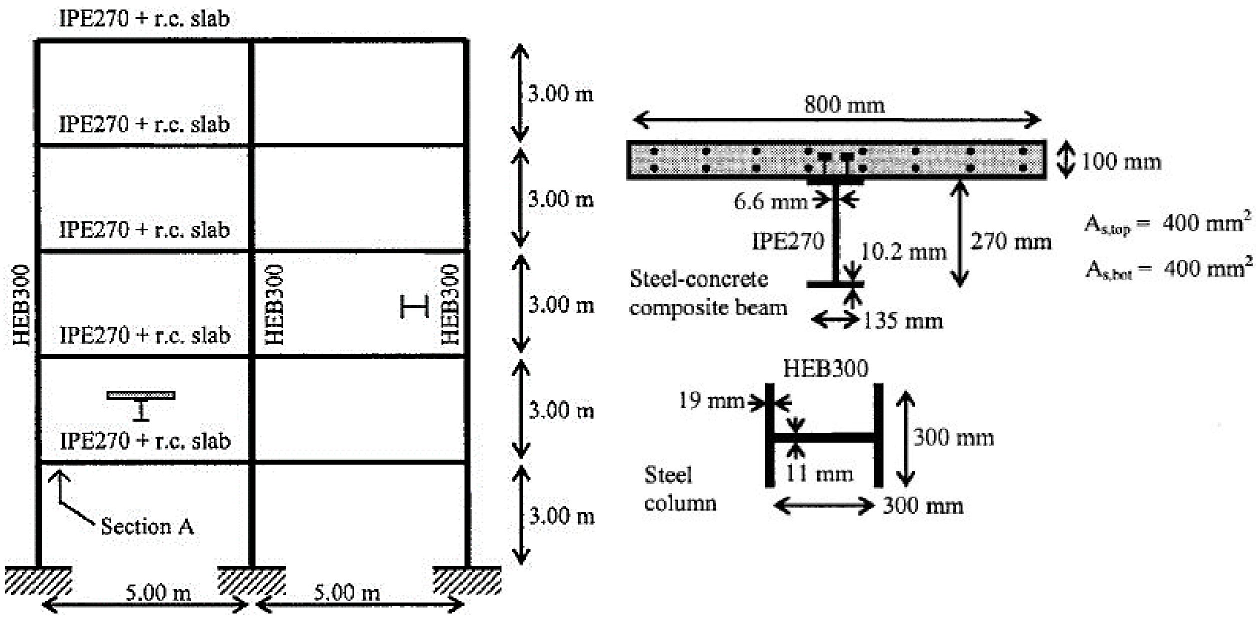

a) Benchmark building frame b) Cross-section (A) geometry

Figure 17 Steel-concrete composite frame tested (Zona et al. 2008 [33])

In "Model-F", the structural fuses have been introduced. The fuses have been designed by means of a parameter a introduced as a capacity ratio, to achieve their best performance in terms of capacity and energy dissipation, as suggested by (Castiglioni et al. 2012 [30]). The a value relates the resistant capacity of the fuse to the plastic resistance of the cross-section of the composite beam, and can be defined as the capacity ratio of the fuse:

$$a = \frac{M_{max,fuse}}{M_{pl}}$$

Where M_{pl} is the plastic moment resistance of the composite beam, and $M_{max,fuse}$ is the maximum moment that can develop in the fuse section. The a value is set to 0.4, as suggested by (Castiglioni et al. 2012 [30]) based on the re-analysis of the experimental results. In the Model-F, the moment-rotation input diagram of device B (Table 4) has been considered. The two numerical models have been developed with the assumptions previously described in the paper, in terms of material and geometric modelling. Hence using inelastic beam elements with fiber-based formulation allowed to highlight the effectiveness of structural fuses for each structural component. First, a static analysis has been performed to obtain the initial conditions necessary for the dynamic analysis, together with a natural frequency analysis for the evaluation of modal properties of the structures. The modal properties of the two analysed frames are presented herein (Table 7 and Figure 18).

Mode	Period [sec]	PF-X [%]	Sum PF-X [%]
Model-B / First mode	0,72	84,1	84,1
Model-B / Second mode	0,23	10,2	94,3
Model-F / First mode	0,76	83,2	83,2
Model-F / Second mode	0,23	10,6	93,8

Table 7 Modes of free vibration

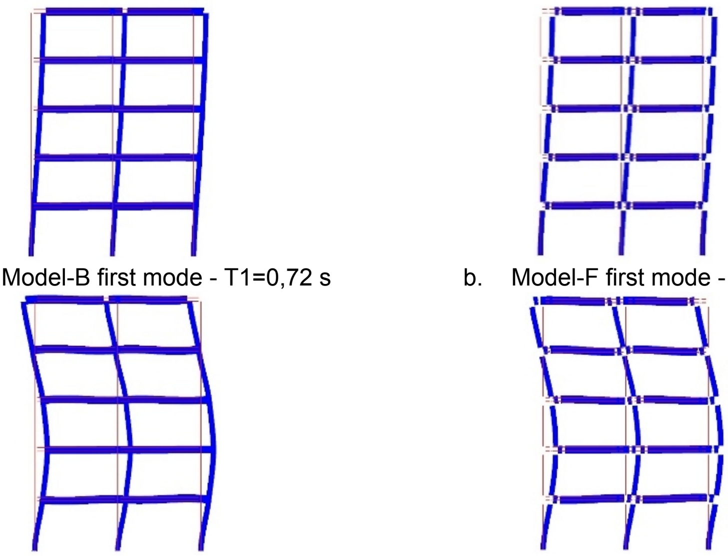

a. Model-B first mode - T1=0,72 s

b. Model-F first mode - T1=0,76 s

c. Model-B second mode - T2=0,23 s

d. Model-F second mode - T2=0,23 s

Figure 18 Modes of free vibration - without structural fuses

For the nonlinear dynamic analyses, three artificial accelerograms have been generated with Gosca software (Denoël V., 2001 [50]), compatible with the design criteria of the structural frame analysed by (Zona et al. 2008 [33]), by using a peak ground acceleration=0.35 g, Type 1 spectrum of EN1998-1-1, modal damping ratio=5%, and soil class B. The use of a set of accelerograms coherent with a Uniform Hazard Spectrum allows to greatly simplify the selection phase, without losing in terms of precision, as already highlighted in several past researches, such as in (Morelli et al. 2018 [51]). In order to observe residual displacements and inter-storey drifts in the structure after the seismic excitation, the accelerograms have the last 5 seconds with acceleration set to zero (The values at the end of the analysis will be referred in the results). Response spectra and the artificial accelerograms are shown in Figure 19 and Figure 20 respectively.

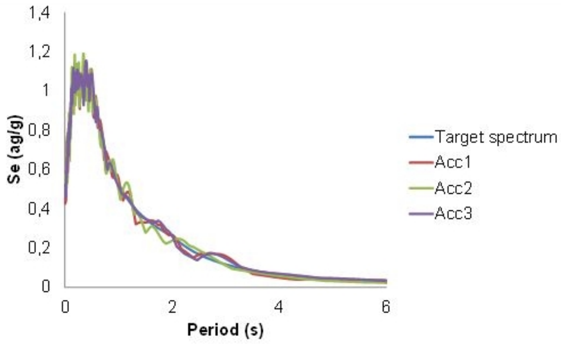

Figure 19 Response spectra for 0,35g, Type 1, soil type B, Damping ratio 5%.

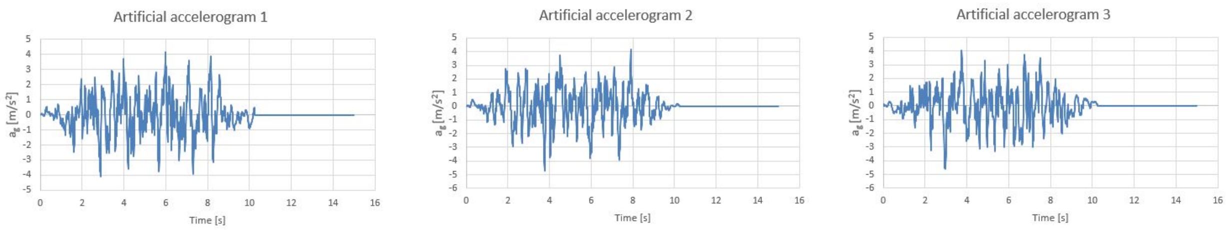

Figure 20 Artificial accelerograms used in the analysis.

The results obtained from each three record are presented below. Since only three accelerograms have been used, the performance of the systems should be interpreted considering the maximum or minimum values. Figure 21 shows the nonlinear behaviour of the structural members of Model-B and Model-F. The inelastic deformations observed in the structural elements have been represented by means of a yield index (changing between 0 and 1.00, being 1.00 fully plastic cross section). As concerns Model-B, in all three analyses, inelastic deformation takes place in the columns at the base level, at the upper levels of the central column and in most of the composite beam elements. These results actually confirm the principles of “capacity design” approach, which represents the desired behaviour for conventional earthquake resistant structures. However, the damage in the structural members caused by the inelastic deformations in this case would not be easily reparable, as discussed previously in this paper. On the other hand, in Model-F, inelastic deformations mainly took place in the structural fuses, while steel beams and columns showed almost elastic behaviour with no significant yielding except in the column at the base level and in the concrete slab due to tension cracks.

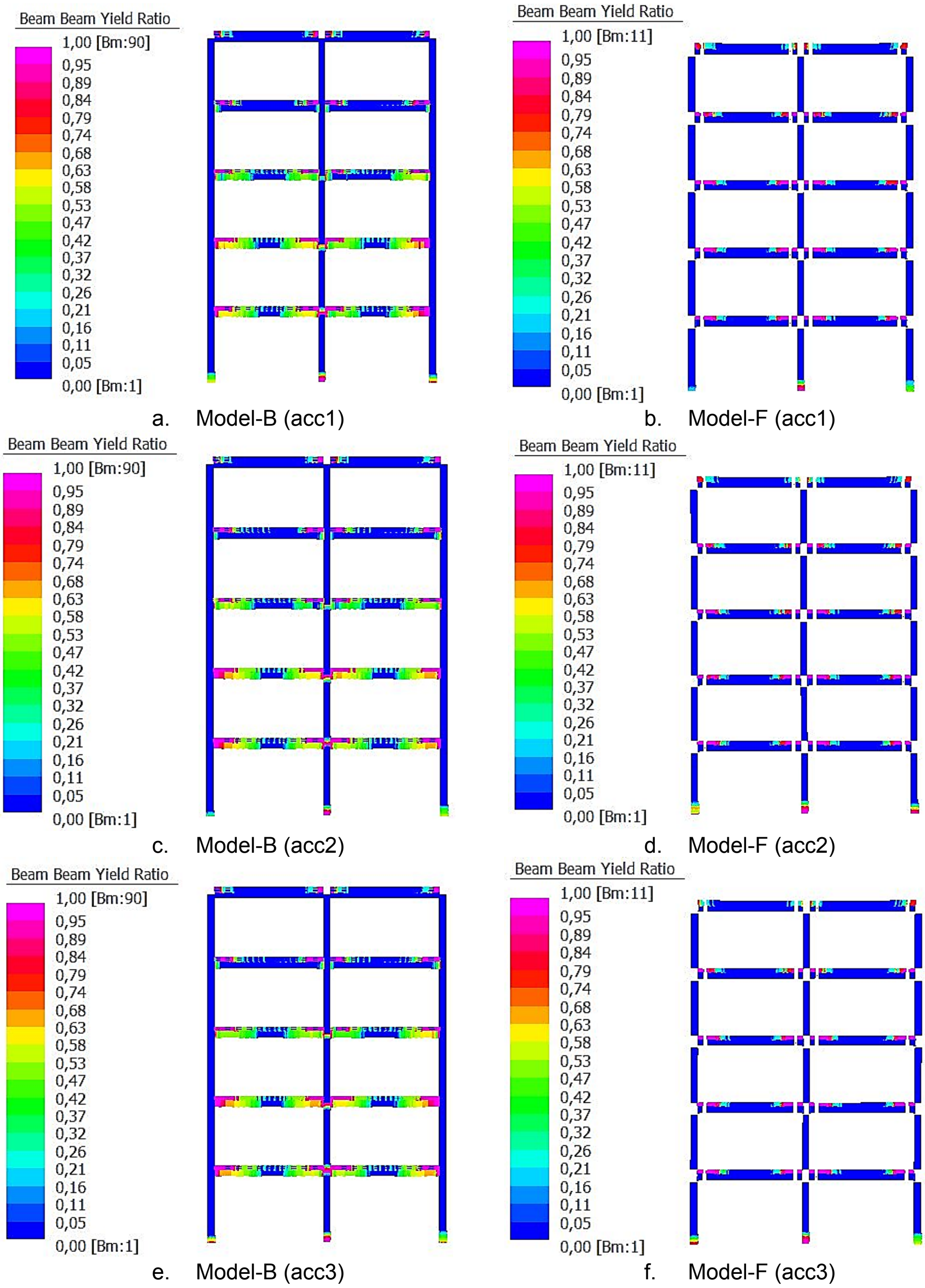

Figure 21 Yield ratio of two models under three accelerograms

The two models have been compared also in terms of floor displacements, inter-storey drift (described as the difference in lateral displacements between two floors normalized by the story height), and base shear, which were the main indicators of the global performance (Figure 22 to Figure 25). It can be observed that Model-B suffers from non-homogeneous distribution of floor displacements and large inter-storey drifts, which indicate the presence of damage to both structural and non-structural components, and potential of a “soft-storey” mechanism. The displacement diagrams show that Model-F reaches higher displacements than those of the Model-

B. This is a consequence of the reduced lateral stiffness of the frame with structural fuses, which can also be observed from the results of model analysis shown in Table 7. On the other hand, after the seismic event (shown by the last 5 seconds of the time-acceleration history diagram), the residual inter-storey drifts remain insignificant for Model-F (0.05 %) (Figure 23.b,d,f), while they are in the order of 1% in case of Model-B (Figure 23.a,c,e). The negligible residual inter-storey drifts (i.e. permanent deformations), showing the re-centering capacity of Model-F, assumes a primary importance for the repair works after the earthquake.

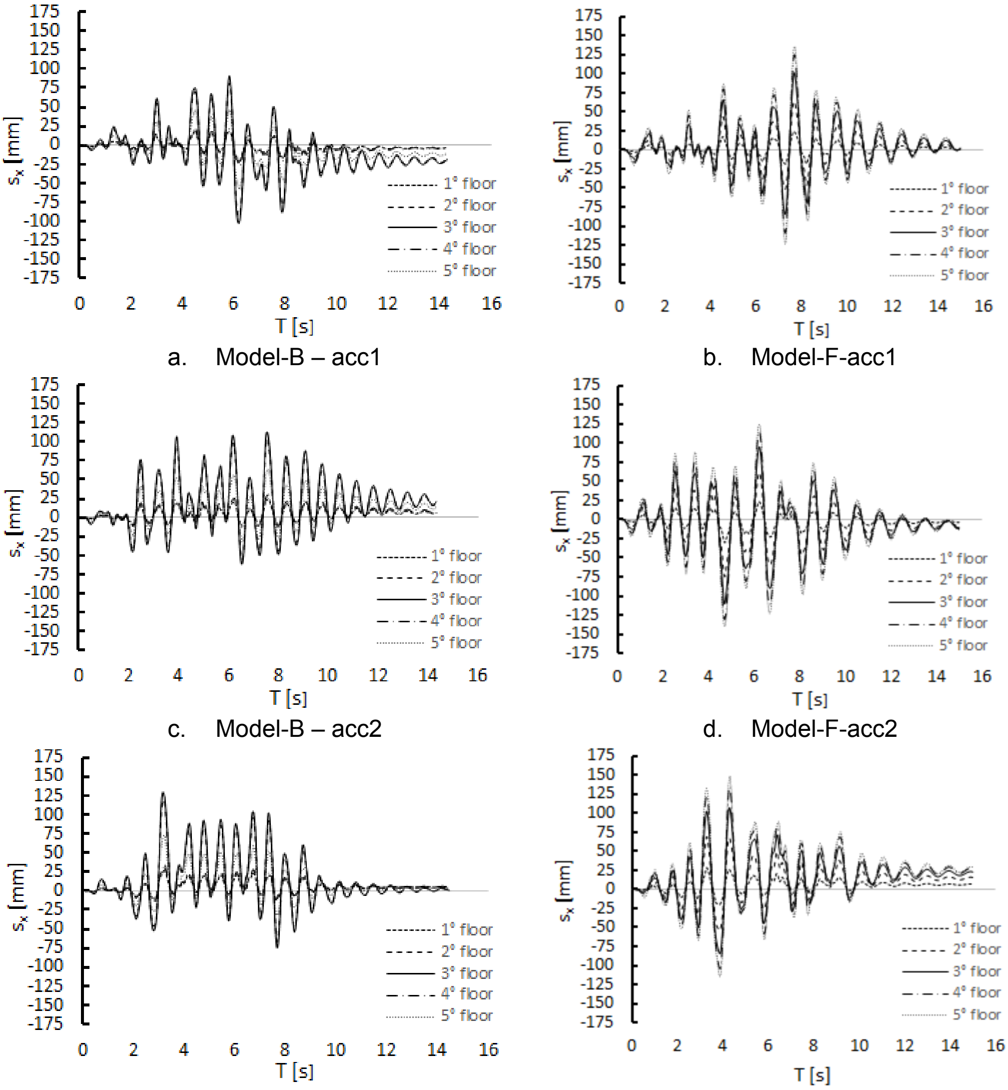

a. Model-B – acc1
b. Model-F-acc1
c. Model-B – acc2
d. Model-F-acc2
e. Model-B – acc3
f. Model-F-acc3

Figure 22 Floor displacements of two models under three accelerograms

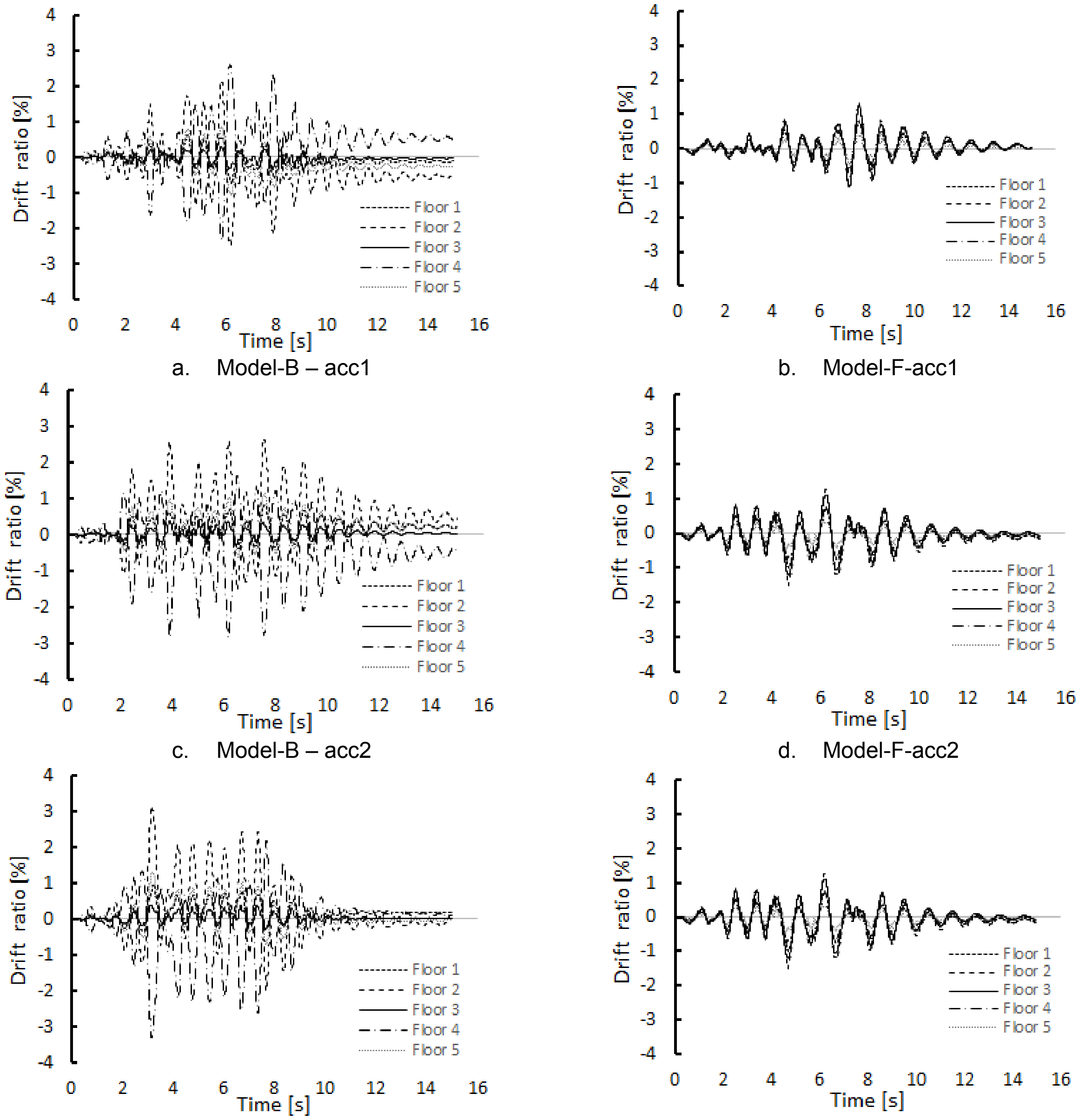

a. Model-B – acc1

b. Model-F-acc1

c. Model-B – acc2

d. Model-F-acc2

e. Model-B – acc3

f. Model-F-acc3

Figure 23 Inter-storey drift ratio of two models under three accelerograms

Figure 24 shows the reduction of maximum base shear forces that takes place in the building with structural fuses.

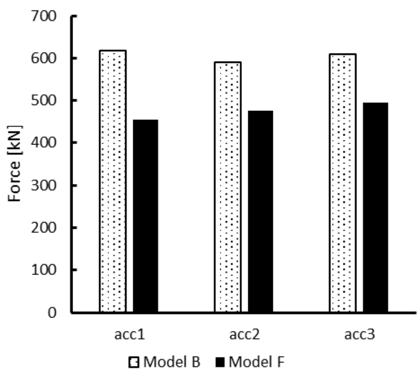

Figure 24 Maximum base shear forces comparison

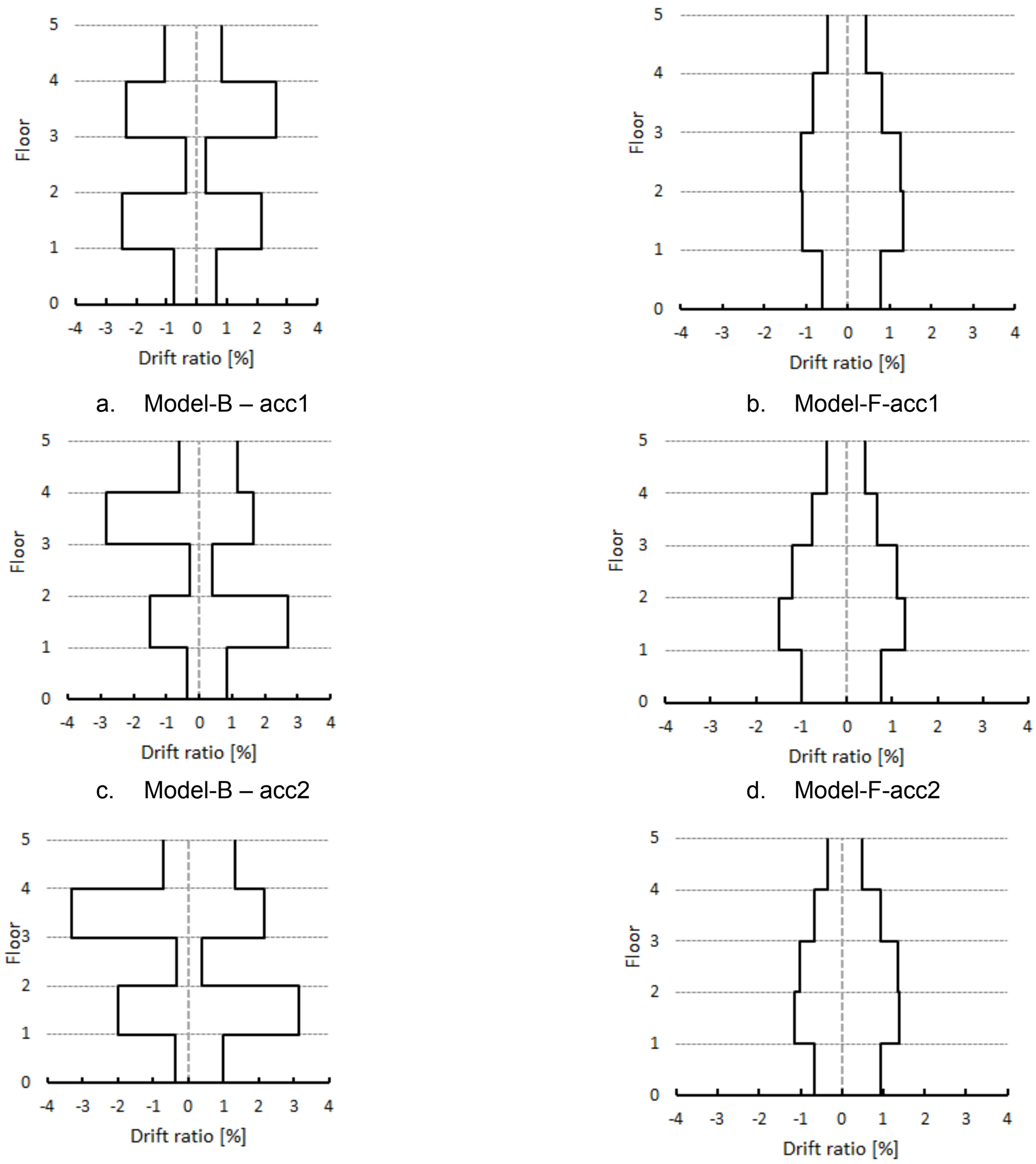

a. Model-B – acc1 b. Model-F-acc1

c. Model-B – acc2 d. Model-F-acc2

e. Model-B – acc3 f. Model-F-acc3

Figure 25 Peak inter-storey drift ratio of MODEL-B and FUSE under three accelerograms

Benefiting from the distributed plasticity numerical approach, it was possible to measure the energy dissipation for each component of the structural system, namely: structural fuses, steel columns and beams, concrete slab, and steel reinforcement bars. This allowed to get more insight on the redistribution of energy in the case of employing structural fuses with respect to the conventional building. The dissipated energy has been calculated based on the areas of the hysteresis diagrams of each plasticized element. Figure 26 classifies the dissipated energy in terms of their sources in the structural frame. In the case of Model-F, the majority of damage takes place in the fuses that can be easily replaced, whereas in the other elements the energy dissipation is drastically reduced. Composite slab dissipates very little energy, which is mainly due to the tension cracks. Steel reinforcement bars remain entirely elastic. In general, comparison between Model-B and Model-F indicate that the latter minimizes the inelastic deformation in the main structural components.The beneficial effect of the fuse device is shown in Figure 26 as comparison of energy dissipation. Figure 26.a indicates maximum energy dissipation is mainly concentrated in the steel beam whereas, the Figure 26.b suggests that the energy dissipation predominantly takes place in the fuse device.

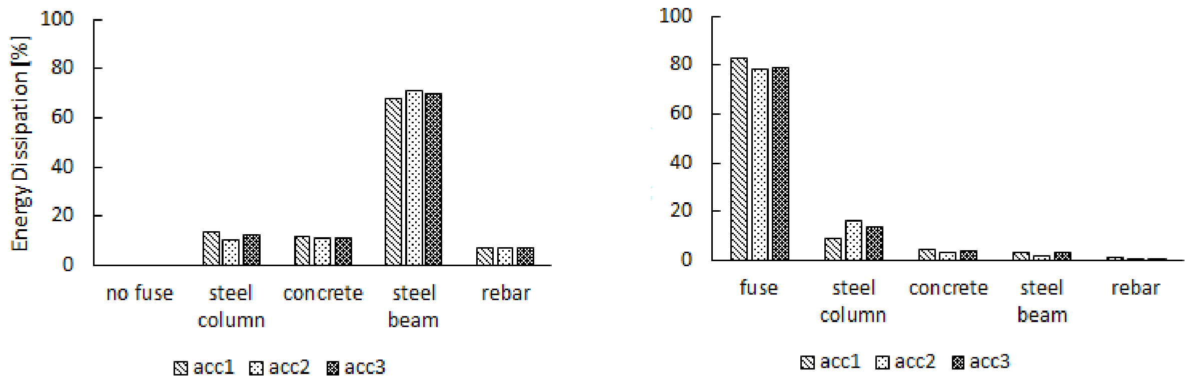

a. Model-B b. Model-F

Figure 26 Comparison of % energy dissipation of building components

5 DISCUSSIONS ON THE REPARABILITY ASPECT

The results of the numerical analysis can be interpreted to show that the structural fuses would enable long-term use of the structural elements of the steel-concrete composite buildings. This improves the sustainability of these types of structures, eliminating the demolition risk after strong earthquake events. This aspect was indeed one of the long-term objectives of European Union in the steel construction sector (European Commission, 2017 [51]). From the benchmark numerical analysis, it is seen that the main objective has been achieved concentrating the seismic damage in the fuses, the rest of the structure remaining essentially elastic. This can be observed from Figure 27, where a comparison is shown between Model-B and Model-F hysteresis curves regarding the base-shear vs 2nd inter-storey drift relation under the three time-history acceleration data. While in Model-B, a large energy dissipation occurred in the 2nd storey structural elements, in Model-F, a smaller energy dissipation occurred, which is also mainly concentrated in the structural fuses present inside the frame. This evidences that the model with structural fuses is much less prone to the “soft-storey” behaviour. Furthermore, the improved re-centering capability of model F can be seen in these graphs, from the accumulation of inter-storey drifts around the origin (in contrary to the Model-B, where a shift is evident in the inter-storey drift axis).

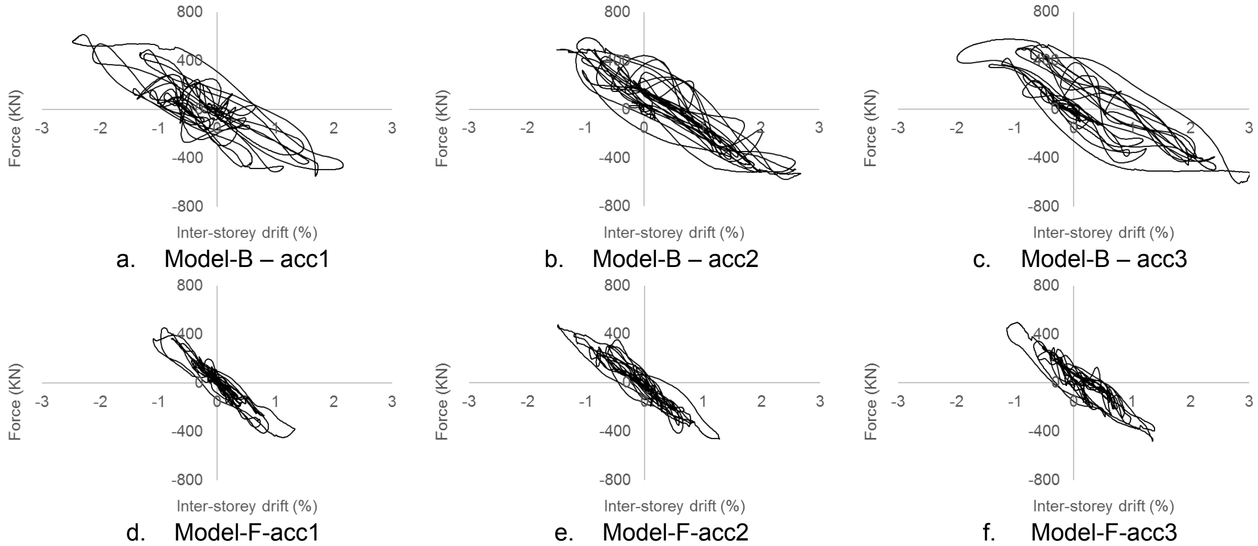

Figure 27 Force vs 2nd inter-storey drift hysteresis curves of FUSE and MODEL-B frames

The capability of the structural fuses to absorb the seismic energy can be quantified with reference to a λ parameter which is the ratio between stored and spent energy according to the sketch shown in Figure 28 and to the total strain energy definition of (Ellyin, F. 1989 [53]). Table 8 compares the percentage of the energy stored in the structural elements excluding the fuses, for the two cases. The percentage of the recoverable energy was 17% and 46%, respectively for the Model-B and Model-F. This shows the larger capability of the Model-F to restore the seismic energy resulting in a higher degree of re-centering.

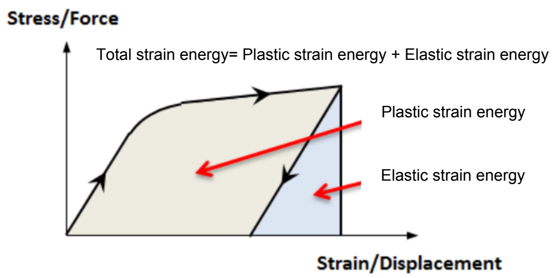

Total strain energy: The total energy expended by the structure
Elastic strain energy: The recoverable energy upon unloading

$$\lambda: \quad \frac{Elastic\ strain\ energy}{Total\ strain\ energy}$$

Figure 28 Stored vs total energy

	Acc1	Acc2	Acc3	Average
λ – Model-F	0.59	0.34	0.44	0.46
λ – Model-B	0.19	0.16	0.16	0.17

Table 8 λ values for two cases

Thanks to this smart redistribution of damage, repair work of such a frame could be achieved easily and efficiently, as was proven during the experimental tests (Figure 29). Replacement of the fuses after testing up to failure was easily performed by two workmen in approximately 30 min/fuse. This tested replacement approach can be also applied in multi-storey buildings. Since the structural elements are not significantly damaged after severe loading conditions, an extension of their lifetime is a direct consequence as well as an increased resilience of the building.

Figure 29 Repair operation after the full-scale tests

These observations have been obtained in a laboratory environment, with ideal working conditions that may not reflect the construction practice. In order to prove the efficacy of the system in the real environment, two authors of this paper (Kanyilmaz and Castiglioni) have been coordinating an EU-RFCS pilot-demonstration project “DISSIPABLE”, which started in June 2018. In this project, shake table testing of half scaled 3D buildings under real three-dimensional seismic excitations will be performed at the Laboratory for Earthquake Engineering (LEE) of National University of Athens (NTUA). The following objectives of this project will be complementary to the conclusions of this paper:

- The adequacy of repair measures of the pilot buildings will be demonstrated.
- The ability of the repaired pilot buildings to continue withstanding other strong earthquakes events will be demonstrated.
- Several non-symmetric arrangements of the resisting elements (stiffness eccentricity) or non-symmetric distribution of masses which produce a torsional response on the global system will be investigated on the pilot buildings.
- Design guidelines will be established based on the results of the experiments and the numerical analyses. The proposed design methodology will be suitable for use in everyday practice.
- A systematic “assembly, removal, repair and reassembly” operative procedure for the dissipative devices will be developed in order to facilitate their adoption and application in current practice.
- Worked examples will be drafted for practical use.
- Case studies will be investigated in order to quantify recyclability and economic aspects.
- A clear comparison will be made between conventional and innovative building costs.

- Environmental and economic life cycle impacts of the fuses will be calculated and compared with existing functional equivalent solutions.
- A comparative life cycle balance will also be performed for the whole building, including non-structural elements, in order to quantify environmental and economic savings of an entire real building due to absence of damage in both structural and non-structural elements. These comparative studies will serve to assess the effectiveness of various loss-reduction measures and determine why and how the proposed system is more resilient than others.

6 CONCLUSIONS

The popularity of dissipative building components has greatly increased within the last two decades. The introduction of these components aims to dissipate the seismic energy through their plastic deformation, leaving main structural elements damaged at a low level. The focus has been given so far to maximize the dissipation capacities of these components, and reparability aspect is mostly neglected. Since it is crucial to restore buildings and its functions as quickly as possible after an earthquake, it is strongly advisable to develop structural systems that are simple to repair. Besides this, most of the existing studies regarding the dissipative components in steel buildings ignore the presence of the reinforced concrete slab.

This paper presented a numerical study on “bolted dissipative beam splices”, also called as “structural fuses” developed in the European Research Project “FUSEIS”. When they are introduced in steel-concrete composite moment resisting frame buildings, the earthquake damage concentrates mainly in the fuses, which can be easily and inexpensively replaced after strong seismic events. The seismic performance of a benchmark steel-concrete composite frame model (Zona, et al., 2008) has been studied with and without structural fuses, taking explicitly into account the reinforced concrete slab in the numerical models. These models have been developed using fiber-based distributed plasticity approach and calibrated based on the experiments provided in the literature and performed in the FUSEIS research project.

The energy dissipated by each component of a steel-concrete composite frame has been quantified, showing its redistribution for both conventional and innovative cases. Results showed that the structural fuses improved the seismic performance in terms of inter-storey drift, energy dissipation and re-centering features. The damage has been concentrated mainly on these connection components, whereas the other frame members suffered very low damage. Conventional frame suffered from large inter-storey drifts and non-homogenous distribution of floor displacements, indicating damage to both structural and non-structural elements, furthermore a high risk of soft-storey mechanism. In case of the building with the structural fuses, these were not present. The residual inter-storey drifts were minimized down to 0.05 % thanks to the structural fuses, from 1% developed in the case of conventional frame, which is an indicator of the possibility of limited repair works after a seismic event.

7 REFERENCES

[1] Engelhardt M.D. and Sabol, T. (1997) 'Seismic-resistant steel moment connections: developments since the 1994 Northridge earthquake', *Prog Struct Mater Eng*, 1(1), pp. 68–77.

[2] Engelhardt, M. D., Sabol, T. A., Aboutaha, R. S. and Frank, K. H. (1995) 'An Overview of the AISC Northridge Moment Connection Test Program', in *Proceeding 1995 National Steel Construction Conference. San Antonio*, 17-19 May: American Institute of Steel Construction.

[3] Popov, E. P., Blondet, M., Stepanov, L. and Stojadinovic, B. (1996) 'Full-Scale Beam-to-Column Connection Tests', SAC Report 1-1, *University of California Department of Civil Engineering, Berkeley.*

[4] Whittaker, A., Bertero, V. and Gilani, A. (1996) 'Seismic Testing of Full-Scale Steel Beam-Column Assemblies', Experimental Investigation of Beam-Column Assemblies, Technical report SAC96-01, pp. 96–01.

[5] Kaufman, E. J. and Fisher, J. W. (1995) 'A study of the effects of material and welding factors on moment frame weld joint performance using a small-scale tension specimen', *SAC Joint Venture*, pp. 95–08.

[6] Krawinkler, H. (1995) 'Earthquake design and performance of steel structures'*, Bulletin-New Zealand National Society for Earthquake Engineering*, 29, pp. 229–241.

[7] Plumier, A. (1990) 'New idea for safe structures in seismic zones', in *IABSE Symposium. Mixed structures including new materials-Brussels*, pp. 431–436.

[8] Yu, Q.-S. K. and Uang, C.-M. (2001) 'Effects of near-fault loading and lateral bracing on the behavior of RBS moment connections', *Steel and Composite Structures*, 1(1), pp. 145–158.

[9] Pachoumis, D. T., Galoussis, E. G., Kalfas, C. N. and Efthimiou, I. Z. (2010) 'Cyclic performance of steel moment-resisting connections with reduced beam sections—experimental analysis and finite element model simulation', *Engineering Structures*, 32(9), pp. 2683–2692.

[10] Avgerinou, S., Lignos, X., Thanopoulos, P., Spiliopoulos, A., Vayas, I., Moment-resisting-frames under cyclic loading: Large scale tests and validation of plasticity and damage numerical models (2018) Soil Dynamics and Earthquake Engineering, 115, pp. 564-577. DOI: 10.1016/j.soildyn.2018.08.036

[11] Plumier, A. (1997) 'The dogbone: Back to the future', *Engineering Journal*, 34 (2), pp. 61-67.

[12] Dubina, D., Stratan, A. and Dinu, F. (2008) ‘Dual high-strength steel eccentrically braced frames with removable links’, *Earthquake Engineering and Structural Dynamics*, 37(15), pp. 1703-1720.
[13] Chan W.K. and Albermani F. (2008) ‘Experimental study of steel slit damper for passive energy dissipation’, *Engineering Structures*, 30(4), pp. 1058-1066.
[14] Gowda K.K and Kiran K.K. (2013) ‘Earthquake resistance of structures using dampers - a review’, *Int. J. Adv. Struct. Geotech. Eng.,* 2(1), pp. 31–35.
[15] Braconi, A., Morelli, F. and Salvatore, W., (2012) ‘Development, design and experimental validation of a steel self-centering device (SSCD) for seismic protection of buildings". Bulletin of Earthquake Engineering, 10 (6), 1915 – 1941.
[16] F. Morelli, N. Mussini, W. Salvatore. "Numerical Model and Experimental Behavior of a Dissipative Steel Frame with Reinforced Concrete Infill Wall". Bulletin of Earthquake Engineering, DOI 10.1007/s10518-018-0475-9.
[17] Morelli F., Manfredi M. and Salvatore W. (2016), ‘An Enhanced Component Based Model of Steel Connection in a Hybrid Coupled Shear Wall Structure: Development, Calibration And Experimental Validation’, *Computers and Structures,* 176, 50–69, DOI: http://dx.doi.org/10.1016/j.compstruc.2016.08.002.
[18] Karavasilis, T.L. (2016) ‘Assessment of capacity design of columns in steel moment resisting frames with viscous dampers’, *Soil Dynamics and Earthquake Engineering*, 88, pp. 215-222.
[19] Hwang, S.-H., Lignos, D.G. Earthquake-induced loss assessment of steel frame buildings with special moment frames designed in highly seismic regions (2017) Earthquake Engineering and Structural Dynamics, 46 (13), pp. 2141-2162. 10.1002/eqe.2898
[20] Kamperidis, V.C., Karavasilis, T.L., Vasdravellis, G. Self-centering steel column base with metallic energy dissipation devices (2018) Journal of Constructional Steel Research, 149, pp. 14-30. DOI: 10.1016/j.jcsr.2018.06.02
[21] Dall'Asta, A., Leoni, G., Morelli, F., Salvatore, W. and Zona, A. (2017) ‘An innovative seismic-resistant steel frame with reinforced concrete infill walls’, *Engineering Structures*, 141, pp. 144-158.
[22] Morelli, F., Piscini, A. and Salvatore, W. (2017) ‘Seismic behavior of an industrial steel structure retrofitted with self-centering hysteretic dampers’, *Journal of Constructional Steel Research*, 139, pp. 157-175.
[23] Vamvatsikos, D. , Castiglioni, C. , Bakalis, K. , Calado, L. , D'Aniello, M. , Degee, H. , Hoffmeister, B. , Pinkawa, M. , Proenca, J. M., Kanyilmaz, A. , Morelli, F. , Stratan, A. and Vayas, I. (2017), I.11.47: A risk‐consistent approach to determine behavior factors for innovative steel lateral load resisting systems. ce/papers, 1: 3434-3443. doi:10.1002/cepa.398

[24] Latour, M., D'Aniello, M., Zimbru, M., Rizzano, G., Piluso, V., Landolfo, R. Removable friction dampers for low-damage steel beam-to-column joints (2018) Soil Dynamics and Earthquake Engineering, 115, pp. 66-81. DOI: 10.1016/j.soildyn.2018.08.002
[25] Piluso, V., Montuori, R., Troisi, M. Innovative structural details in MR-frames for free from damage structures (2014) Mechanics Research Communications, 58, pp. 146-156. Cited 40 times. doi: 10.1016/j.mechrescom.2014.04.002
[26] Vayas, I. (2017) 'Innovative anti-seismic devices and systems', *ECCS European Convention for Constructional Steelwork*, ISBN: 978-92-9147-136-2
[27] INNOSEIS EU-RFCS 7210-PR-316, http://innoseis.ntua.gr/
[28] Vayas, I., Karydakis, P., Dimakogianni, D., Dougka, G., Castiglioni, C., Kanyilmaz, A., Calado, L., Proença, J. M., Espinha, M., Hoffmeister, B., Rauert, T. and Kalteziotis, D. (2013) 'Structural fuses for seismic-resistant steel frames', *Final Report EUR 25901 EN. Brussels*.
[29] Calado, L., Proença, J. M., Espinha, M. and Castiglioni, C. A. (2013) 'Hysteretic behaviour of dissipative bolted fuses for earthquake resistant steel frames', *Journal of Constructional Steel Research*, 85, pp. 151–162.
[30] Castiglioni, C. A., Kanyilmaz, A. and Calado, L. (2012) 'Experimental analysis of seismic resistant composite steel frames with structural fuses', *Journal of Constructional Steel Research*, 76, pp. 1–12.
[31] Dimakoyianni, D., Dougka, G. and Vayas, I. (2015) 'Seismic behavior of frames with innovative energy dissipation systems (FUSEIS1-2)', *Engineering Structures,* 90, pp. 83–95.
[32] Dougka, G., Dimakogianni, D. and Vayas, I., (2014) 'Innovative energy dissipation systems (FUSEIS 1-1) - Experimental analysis', *Journal of Constructional Steel Research*, 96, pp. 69-80.
[33] Zona, A., Barbato, M. and Conte, J. P. (2008) 'Nonlinear seismic response analysis of steel–concrete composite frames', *Journal of structural engineering*, 134(6), pp. 986–997.
[34] Uriz, P. (2008) 'Toward earthquake-resistant design of concentrically braced steel-frame structures'. *Berkeley, Calif. : Pacific Earthquake Engineering Research Center.*
[35] Sabelli, R. (2001) 'Research on improving the design and analysis of earthquake-resistant steel-braced frames', *NEHRP Prof Fellowship Report EERI*, pp. 1–142.
[36] Nie, J. and Cai, C. S. (2003) 'Steel-concrete composite beams considering shear slip effects', *Journal of Structural Engineering*, 129(4), pp. 495–506.
[37] Bursi, O. S. and Gramola, G. (2000) 'Behaviour of composite substructures with full and partial shear connection under quasi-static cyclic and pseudo-dynamic displacements', *Materials and Structures*, 33(3), pp. 154–163.
[38] Nie, J., Tao, M., Cai, C. S. and Chen, G. (2011) 'Modeling and investigation of elasto-plastic behavior of steel–concrete composite frame systems', *Journal of Constructional Steel Research*, 67(12), pp. 1973–1984.

[39] Valente, M., Castiglioni, C.A. and Kanyilmaz, A. (2016) ‘Dissipative devices for earthquake resistant composite steel structures: bolted versus welded solution’ *Bulletin of Earthquake Engineering*, 14(12), pp. 3613-3639.

[40] Valente, M., Castiglioni, C.A. and Kanyilmaz, A. (2017) ‘Numerical investigations of repairable dissipative bolted fuses for earthquake resistant composite steel frames’, *Engineering Structures*, 131, pp. 275-292.

[41] Valente, M., Castiglioni, C.A. and Kanyilmaz, A. (2017) ‘Welded fuses for dissipative beam-to-column connections of composite steel frames: Numerical analyses’ *Journal of Constructional Steel Research*, 128, pp. 498-511.

[42] Straus7 Manual (2004) *Theoretical Manual - Theoretical background to the Straus7 Finite Element analysis system*. Release 2.3. G+D Computing.

[43] Nguyen P. and Kim S. (2014) ‘Distributed plasticity approach for time-history analysis of steel frames including nonlinear connections’ *Journal of Constructional Steel Research*, 100, pp. 36-49, ISSN 0143-974X

[44] UNI EN 1992 (2004) ‘Eurocode 2: Design of Concrete Structures: Part 1-1: General Rules and Rules for Buildings’, *British Standards Institution.*

[45] Udagawa, K. and Mimura, H. (1991) ‘Behavior of composite beam frame by pseudodynamic testing’, *Journal of Structural Engineering*, 117(5), pp. 1317–1334.

[46] Vayas, I., Dimakogianni, K. D., Dougka, G., Castiglioni, C. A., Kanyilmaz, A. and others (2012a) ‘Structural fuses for seismic resistant steel frames-The FUSEIS Project, Design Guide’, *Research Programme of the Research Fund for Coal and Steel*.

[47] Takeda, T., Sozen, M. A. and Nielsen, N. N. (1970) ‘Reinforced concrete response to simulated earthquakes’, *Journal of the Structural Division*, 96(12), pp. 2557–2573.

[48] UNI EN 1994-1-1 (2004) ‘Eurocode 4: Design of composite steel and concrete structures - Part1-1: General rules and rules for buildings’. Brussels: European Committee for Standardization.

[49] UNI EN 1998-1 (2005) *Eurocode 8–Design of Structures for earthquake resistance–Part 1: General rules, seismic actions and rules for buildings*. Brussels: *European Committee for Standardization*.

[50] Denoël, V. (2001) ‘Generation of Spectrum Compatible Accelerograms (GOSCA)’, *Université* de Liège, Belgique.

[51] Morelli, F., Laguardia, R., Faggella, M. et al. Ground motions and scaling techniques for 3D performance based seismic assessment of an industrial steel structure". Bulletin of Earthquake Engineering. DOI 10.1007/s10518-017-0244-1.

[52] European Parliament, and the Council “Directive 2008/ 98/EC of the European parliament and of the council of 19 November 2008 on waste and repealing certain directives”, Official Journal

of the European Comission 2017, The Future of European Steel, Innovation and sustainability in a competitive world and EU circular economy, doi: 10-2777/51833 KI-01-17-365-EN-N.

[53] Ellyin F. (1989) ‘Cyclic Strain Energy Density as a Criterion for Multiaxial Fatigue Failure, Biaxial and Multiaxial Fatigue, EGF3’, *Mechanical Engineering Publications*, pp. 571-583